PEER-REVIEWED ARTICLE

Satellite imagery for hazard detection: better use of satellite imagery could help prevent groundings in the Canadian Arctic

Author
Anders Knudby[1,2]

Abstract
This study demonstrates how satellite imagery can reduce the risk of grounding in poorly surveyed waters. Automated shoal detection and satellite-derived bathymetry (SDB) were applied to Sentinel-2 imagery for seven grounding sites in the Canadian Arctic. Shoal detection was successful for all sites, and SDB showed depths as shallow as 0.3 m. Proactive use of satellite imagery, even without advanced image processing, could have provided mariners with vital information on the location of uncharted shoals and prevented costly and dangerous accidents. The hydrographic community should accelerate the inclusion of satellite-derived products into the information provided to mariners for safety of navigation.

Keywords
satellite imagery · satellite-derived bathymetry · shoal detection · groundings · Canadian Arctic

Resumé
Cette étude démontre comment l'imagerie satellitaire peut contribuer à réduire le risque d'échouement dans les eaux faiblement hydrographiées. La détection automatisée des hauts-fonds et la bathymétrie dérivée par satellite (SDB) ont été appliquées à l'imagerie Sentinel-2 pour sept sites d'échouement dans l'Arctique canadien. La détection des hauts-fonds a été couronnée de succès pour tous les sites, et la SDB a montré des profondeurs aussi faibles que 0,3 m. L'utilisation proactive de l'imagerie satellite, même sans traitement d'image avancé, aurait pu fournir aux navigateurs des informations vitales sur l'emplacement des hauts-fonds non cartographiés et éviter des accidents coûteux et dangereux. La communauté hydrographique devrait accélérer l'intégration des produits dérivés des satellites dans les informations fournies aux navigateurs pour la sécurité de la navigation.

✉ Anders Knudby · aknudby@uottawa.ca
[1] University of Ottawa, Department of Geography, Environment and Geomatics, Ottawa, ON K1N 6N5, Canada
[2] Liquid Geomatics Ltd., Ottawa, ON, K1S 0T3, Canada

https://doi.org/10.58440/ihr-31-2-a13

Resumen

Este estudio demuestra cómo las imágenes por satélite pueden reducir el riesgo de tocar fondo en aguas con levantamientos hidrográficos pobres. Se aplicó la detección automatizada de bajos y la batimetría derivada por satélite (SDB) a las imágenes de Sentinel-2 para siete lugares donde se había tocado fondo en el Ártico canadiense. La detección de bajos fue satisfactoria en todos los casos, y SDB mostró profundidades tan someras como 0,3 m. El uso proactivo de imágenes por satélite, incluso sin un procesamiento avanzado de las imágenes, podría haber proporcionado a los navegantes información vital sobre la ubicación de bajos no cartografiados y haber evitado accidentes costosos y peligrosos. La comunidad hidrográfica debería acelerar la inclusión de productos derivados de satélite en la información que se proporciona a los navegantes para la seguridad de la navegación.

1 Introduction

The Arctic Ocean is experiencing profound and rapid climatic changes, with significant implications for sea ice, navigability and maritime transportation. Human-induced warming has accelerated the decline in sea ice extent and thickness (Yadav et al., 2020), lengthening the ice-free season, and projections suggest that the Arctic could experience nearly ice-free summers as early as 2030 (Kim et al., 2023). These changes allow the opening of new shipping routes into and across the Canadian Arctic, routes that are becoming more accessible for longer periods each year (Liu et al., 2024). Recent years have seen an increase in maritime transportation in the Canadian Arctic Ocean (Dawson et al., 2018). In 2024, 466 ship voyages were recorded in Canadian Arctic waters, compared to 301 in 2014, a 55 % increase over the last decade, despite excluding data from November and December 2024 (Lasserre & Baudu, 2024).

However, the Canadian Arctic Ocean remains poorly surveyed and charted. The Canadian Hydrographic Service (CHS) estimates that only 15.8 % of Canadian Arctic waters have been adequately surveyed, including only 44.7 % of key navigational routes, and many charts contain minimal or insufficient information to support safe and efficient navigation (CHS, 2023). Many areas outside shipping corridors contain only outdated survey data, or no data at all, leading charts to be sparsely populated with soundings or simply contain white space with no information. The soundings that do exist can be over 100 years old, created from lead line measurements with positioning based on triangulation to points on land, the locations of which are themselves of unknown accuracy (Government of Canada, 2014). Even the distinction between land and water is sometimes incorrect on older CHS charts. For example, while supporting recent updates to CHS charts 7185 and 7193, the author identified the correct location of an island charted almost 2 km from its actual location, in addition to numerous previously uncharted shoals. An island >500 m across, which had been charted as a shoal, was also identified (Fig. 1). Such incomplete and erroneous charts, combined with increasing production and mobility of icebergs in the Arctic Ocean (Dalton, 2023) and increasing maritime traffic, inevitably create a substantial risk to the safety of navigation in Canada's Arctic (Howell et al., 2024; Nicoll et al., 2024; TSB, 2010).

While groundings are relatively infrequent in the Canadian Arctic due to the small total number of voyages, compared to other marine regions the Arctic has the highest accident rate at ~10 accidents per 1000 commercial ship movements (Council of Canadian Academies, 2016). Approximately 16 % of these are groundings (TSB, 2025). From 2000 to 2018, the Transportation Safety Board of Canada (TSB) received reports of 74 instances of vessel

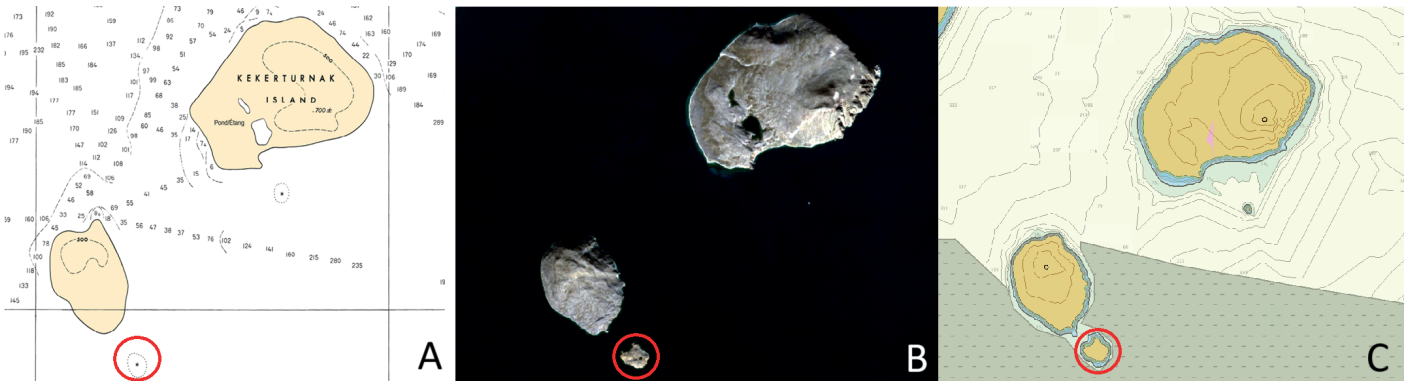


Fig. 1 During work to update CHS chart 7185, a shoal indicated in the chart from 2016 (A) was found in satellite imagery to be an island larger than 500 m across (B), allowing it to be positioned and outlined correctly in the updated chart (C).

grounding or bottom contact in the Canadian Arctic. The severity of these occurrences varies; some vessels sustain little to no damage and simply refloat at high tide, while others result in hull damage and breached fuel tanks, pollution, evacuation of crew and passengers, and high costs for search and rescue, cleanup, and repairs (TSB, 2021). A substantial number of these groundings occur on uncharted shoals; some of these shoals are known to the CHS but not included on charts and instead communicated to mariners through the use of Notices to Shipping (NOTSHIP; TSB, 2010). Others only become known after a grounding has occurred.

Satellite imagery remains underutilized in Canada's Arctic, especially for identifying hazards not included on official charts. While most shoals are not known to CHS in advance of a vessel grounding, many of them are nonetheless easily detectable using satellite imagery. Water is typically clear throughout much of the Arctic Ocean and shoals are often easily visible in optical satellite imagery. This includes free and publicly available imagery such as that provided by the Sentinel-2 MultiSpectral Instrument (MSI), for which imagery has been available for most of the Arctic Ocean since 2015 (Trémas et al., 2015). These shoals can be identified either using automated image processing algorithms (Richardson et al., 2024) or simply by visually inspecting the imagery and delineating the areas where the seafloor is visible. In areas of high turbidity, as is typical in glacial fjords or near river outlets, or under other unsuitable environmental conditions (e.g. in the presence of ice cover, cloud shadowing, whitecaps, or excessive sunglint), detection and delineation of shoals from optical satellite imagery is not always possible. But for large parts of the Arctic Ocean shoals are clearly visible to depths of at least ~10 m.

In addition to delineation of the locations and extents of shoals, a variety of algorithms exist to estimate the depth of water from the colour of the area as observed in a satellite image. These algorithms are collectively known as satellite-derived bathymetry (SDB) and can be used to approximate the depth of shoals. Most SDB algorithms employ one of two approaches. In empirical SDB, trusted geolocated water depth measurements, typically obtained with acoustic or lidar instruments, are used to establish an empirical relationship between pixel colour and water depth. That relationship is then extrapolated to the parts of the image for which water depths are to be estimated (Caballero & Stumpf, 2023; Ilori et al., 2019; Knudby & Richardson, 2023; Lyzenga, 1985, 1978; Stumpf et al., 2003). An alternative approach, often termed physics-based SDB, inverts a radiative transfer model by matching the color observed in each pixel to a set of realistic environmental parameters, including water depth, that it most closely matches (Dekker et al., 2011; Hedley et al., 2012; Knudby et al., 2016; Lee et al., 1999). This approach eliminates the need for trusted geolocated water depths measurements, which often do not exist in the Canadian Arctic, but instead relies on the ability to accurately account for all environmental factors that influence how water depth influences pixel color. Less-used alternative approaches to SDB also exist, including the use of photogrammetry (Hodúl et al., 2020, 2018) and wave-based kinematics (Daly et al., 2022). SDB is increasingly used in production of nautical charts, including by the United Kingdom, France, the United States (Mavraeidopoulos et al., 2017), and more recently Canada (Ahola et al., 2020; Chénier et al., 2018). However, despite the availability of satellite imagery for the entire Canadian Arctic, operational application of SDB has been limited.

The limited bathymetric information displayed on many charts of the Canadian Arctic, contrasted with the wealth of such information available in satellite imagery, suggests that an expanded use of satellite imagery for providing bathymetric information to mariners would be beneficial and could help reduce the frequency of groundings in Canada's increasingly busy Arctic Ocean. In this study, satellite imagery is used for i) shoal detection and ii) SDB, to illustrate the potential for satellite imagery to provide information that could reduce the risk of navigation in poorly charted waters. The study is based on seven cases from the Canadian Arctic Ocean, each featuring a vessel grounding on a shoal that a) is clearly visible in satellite imagery but b) was uncharted at the time of grounding.

2 Data and methods

2.1 Groundings

Relevant case studies were identified using the TSB's publicly available marine transportation occurrences database (TSB, 2025). As of February 2025, the database contained 86124 occurrences from 1975 to 2025 (many entries were duplicates, so the actual number of occurrences is smaller). Occurrences were first filtered to include only those classified as bottom contact or grounding under power, outside a harbor area, and located north of 65 °N, leaving 760 occurrences. Of those, seven were chosen for inclusion in this study based on i) their location in the Canadian Arctic Ocean, ii) the visibility of shoals in satellite imagery, iii) a desire to achieve a geographically distributed set of cases, and iv) other factors, such as weather, that indicate that the groundings could have been avoided if the shoals had been included on CHS charts, and v) the need to focus on a subset of occurrences for investigation. The resulting set of selected groundings is outlined in Table 1 and shown on Fig. 2. As per the criteria listed above, this is not intended to be an exhaustive or representative list of groundings in the Canadian Arctic Ocean. Interested readers are referred to the TSB's official list of occurrences for more examples.

2.2 Satellite imagery and CHS charts

For each grounding site, all Sentinel-2 images

https://doi.org/10.58440/ihr-31-2-a13

available from July to October for the years 2023 and 2024 were accessed, imagery with >50 % cloud cover was removed, and the remaining images were visually assessed to remove those with substantial ice cover, haze, or other environmental conditions rendering them unsuitable for SDB. As a result, between nine and thirteen images were available for each grounding site. The location, date and year of each grounding was used to identify the CHS chart that was current, i.e. the chart that the vessel crew would have had access to, at the time of grounding. These charts were located and accessed from Libraries and Archives Canada and scanned on a large-format scanner. A section of the relevant chart surrounding each grounding site was then manually georeferenced based on distinctive coastline features, using the Sentinel-2 satellite imagery for reference.

2.3 Shoal detection

For shoal detection, a global model for delineation of optically shallow water (Richardson et al., 2024) was applied to the Sentinel-2 images available for each site. For each image, this model produces a per-pixel probability of water being optically shallow, i.e. the probability that the seafloor is visually detectable in the imagery, after applying a mask to exclude non-water pixels. To identify shoals, the mean unmasked value of these per-image probabilities was then calculated, and pixels with a resulting value greater than 50 % were labeled as shoals. Visual examination of the results suggested that this 50 % threshold achieved a good trade-off between limiting false positives (image noise labeled as shoals) and limiting false negatives (undetected shoals).

2.4 Satellite-derived bathymetry

For SDB production, the Fully Automated Bathymetry (FAB) workflow, developed by Liquid Geomatics Ltd. was employed. FAB processing is based on 100 km × 100 km Sentinel-2 image tiles; products for smaller areas such as those surrounding each of the grounding sites illustrated in this paper can be extracted from the larger tiles. FAB processes Sentinel-2A and -2B images end-to-end, including image download from Copernicus Dataspace, land and cloud masking, deglinting (optional), atmospheric correction (Hedley, 2018), bathymetry estimation based on radiative transfer model (RTM) inversion (Hedley et al., 2009), correction for tide level at image acquisition (Lyard et al., 2021), and ensemble predictions based on multiple images for each site (Ilori & Knudby, 2020). FAB is implemented in Python 3.11, with calls to the IDA software (Hedley, 2019) for deglinting, atmospheric correction and RTM inversion (Hedley et al. 2018; Casal et al., 2020). Detailed information on data processing in the FAB workflow is provided in Appendix A.

2.5 SDB accuracy assessment

For most of the grounding sites, no or insufficient acoustic data was available to assess the accuracy of the SDB bathymetry maps produced with FAB. For the two sites where data was available, namely the grounding sites of the *Clipper Adventurer* and *V/L Camsell*, NONNA10 data was downloaded from CHS (CHS, 2024) and reprojected to match the spatial reference system of the relevant Sentinel-2 imagery. Sentinel-2 imagery is distributed projected to WGS-based UTM zones based on the Military Grid Reference System (MGRS). CHS's NONNA data is a set of non-navigational bathymetric survey data, compiled from individual surveys and made publicly available in raster format. For the *Clipper Adventurer* site, most of the NONNA data came

Table 1 List of the seven groundings included in this study, in chronological order.

Vessel name	Date	Location (lat / lon)	Notes	TSB report
Unknown	31 Aug. 1980	77.51 N, 85.48 W	Hull damage sustained, grounding during clear weather and smooth seas.	4287
V/L Camsell	25 Aug. 1984	68.57 N, 99.65 W	Grounding happened in an area of incomplete soundings, during clear weather and smooth seas. Hull damage sustained.	9351
Unknown	24 Aug. 1990	68.13 N, 99.08 W	Grounding happened during search and rescue, clear weather, light ice cover.	18332
Clipper Adventurer	27 Aug. 2010	67.97 N, 112.67 W	128 passengers evacuated. Extensive hull damage, minor fuel oil spill.	M10H0006
Martin Bergmann	03 Sept. 2014	68.40 N, 99.21 W	Grounding happened during search for the lost Franklin ships.	M14C0182
Akademik Ioffe	24 Aug. 2018	69.72 N, 91.35 W	163 passengers and crew evacuated, hull damage and minor fuel oil spill.	M18C0225
Hanse Explorer	23 Aug. 2019	72.58 N, 85.66 W	Passengers onboard, grounding in far northern location.	M19C0276

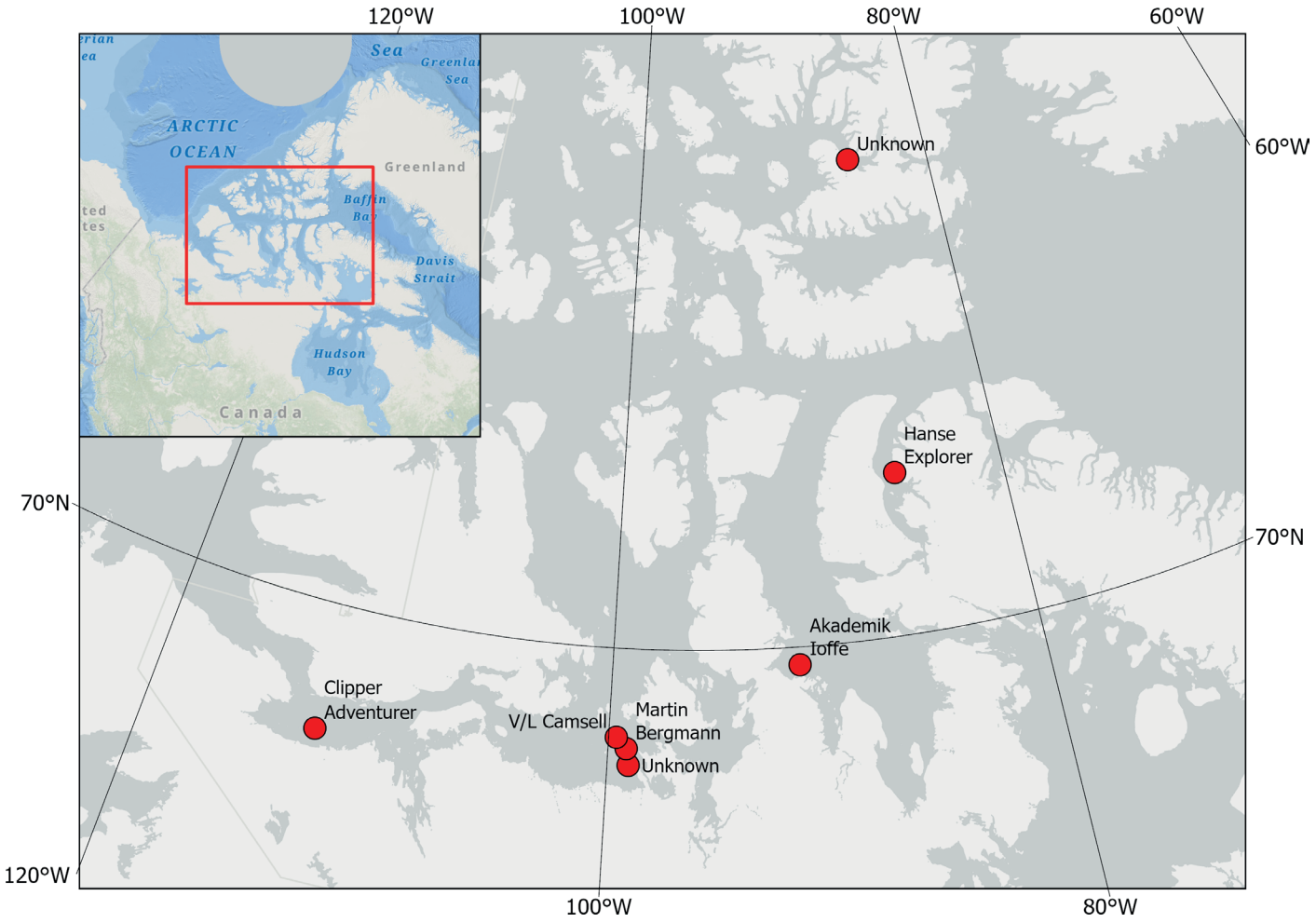


Fig. 2 The locations of the seven groundings used in this study, within the Canadian Arctic Archipelago.

from a 2010 multi-beam survey conducted following the grounding. This survey covered the entire shoal and the immediate surroundings and is categorized as Zone of Confidence (CATZOC) A2. For the *V/L Camsell* site, ~95 % of the NONNA data came from an Airborne Lidar Bathymetry (ALB) survey from 1986 categorized as CATZOC B; a few additional data points came from a single-beam survey conducted sometime between 1955 and 1964, categorized as CATZOC C. Bathymetry was extracted from overlapping SDB and NONNA10 pixels for comparison and calculation of the coefficient of determination (R^2) and the mean absolute difference (MAD) between the two data sets. This comparison was limited to SDB depths <= 10 m, beyond which the accuracy of SDB estimates in this region rapidly degrades due to the decreasing magnitude of the bottom-reflected optical signal recorded in the satellite imagery.

3 Results

3.1 The groundings

Below, a review of i) the CHS chart at the time of grounding, ii) satellite imagery of the grounding site, and iii) the shoal detection and FAB SDB products, is provided for the most recent four groundings listed in Table 1. Similar reviews for the remaining three groundings are provided in Appendix B.

3.1.1 Clipper Adventurer grounding

On 27 August 2010, the *Clipper Adventurer* ran aground on a known but uncharted shoal in Coronation Gulf, Nunavut, during calm seas and with clear visibility. All passengers were uninjured but evacuated from the vessel, and minor pollution was reported. The vessel was successfully refloated after multiple attempts conducted over a ~2-week period (TSB, 2010). Fig. 3 shows a comparison between the relevant subset of the 1990 version of CHS chart 7777, current at the time of the grounding (A), satellite imagery of the area (B, C), the shoal detection product (D), and the FAB SDB product (E). Soundings on the chart appear in a single line passing closely to the northeast of the shoal on which the *Clipper Adventurer* grounded. The shoal is clearly visible in the satellite imagery, identified in the shoal detection product, and the FAB SDB product indicates that it has a minimum depth of 4.0 m. For comparison, the draught of the *Clipper Adventurer* is 4.5 m (forward) and 4.6 m (aft) (TSB, 2010), making prior knowledge of a shoal at 4.0 m depth critically important to navigational decision-making. This particular shoal had actually already been reported in 2007 by

https://doi.org/10.58440/ihr-31-2-a13

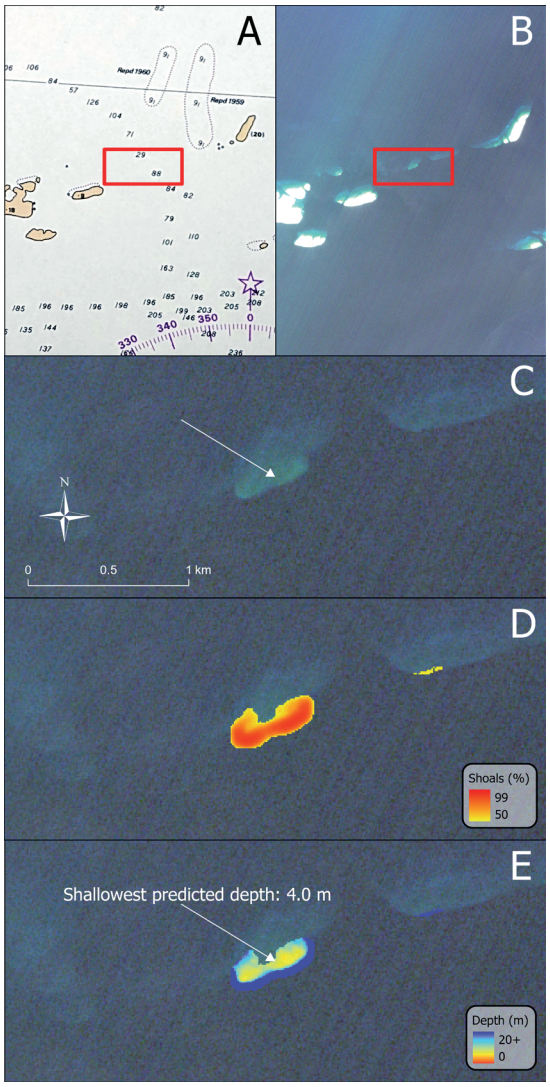


Fig. 3 Comparison of a subset of CHS chart 7777 from 1990, current at the time of grounding (A), a Sentinel-2 satellite image covering the same area (B), a section of the satellite image showing the shoal on which the grounding happened in greater detail (C), the same satellite image with the shoal detection product overlaid (D), and the same satellite image with the FAB SDB product overlaid (E). The extent of the areas shown in (C-E) is indicated by the red rectangles in (A) and (B). Note that the location of the grounding reported by TSB is approximately 500 m SE of the shoal shown here, which was correctly identified on the basis of the CHS survey that followed the grounding.

the Canadian Coast Guard Ship (CCGS) *Sir Wilfrid Laurier*, leading to the publication of a Notice to Shipping (NOTSHIP) that indicated a minimum depth of 3.3 m. However, CHS determined that the information provided from *Sir Wilfrid Laurier* did not meet the requirements for a permanent chart update and instead planned a detailed survey for 2009 to produce data of sufficient quality. Ultimately this did not happen until after the *Clipper Adventurer* grounding in 2010. In the meantime, in 2008, another passenger vessel, the *Akademik Ioffe*, passed near the same shoal. The crews of both vessels were unaware of the NOTSHIP that reported the shoal's existence (TSB, 2010).

3.1.2 Akademik Ioffe grounding

On 24 August 2018, the passenger vessel *Akademik Ioffe* ran aground 78 nautical miles north-northwest of Kugaaruk, Nunavut, in an area almost entirely without charted bathymetric information. The vessel was refloated the same night, and the passengers, all uninjured, were evacuated the next morning. Minor pollution was reported (TSB, 2021). Fig. 4 shows a comparison between the relevant subset of the 1998 version of CHS chart 7502, current at the time of the grounding (A), satellite imagery of the area (B, C), the shoal detection product (D), and the FAB SDB product (E). Two soundings appear on the subset of the chart shown in Fig. 4, indicating depths of 71 and 92 meters respectively, both over 2 km from the shoal on which the *Akademik Ioffe* ran aground. This corresponds to the note on the chart that the charted information is "of a reconnaissance nature collected from CHS spot sounding surveys". The shoal appears faint but is clearly visible in the satellite image, correctly detected by the shoal product, and the FAB SDB product indicates a minimum depth of 4.5 m. The draught of the *Akademik Ioffe* is 5.9 m.

3.1.3 Hanse Explorer grounding

On 23 August 2019, the yacht *Hanse Explorer* ran aground in Admiralty Inlet, Nunavut. No pollution or injuries were reported, and the vessel sustained only minor damage. Approaching Levasseur Inlet, "the under-keel water depth abruptly diminished from 44 m to 0 m and the vessel ran aground" (TSB, 2021). Fig. 5 shows a comparison between the relevant subset of the 1985 version of CHS chart 7568, current at the time of the grounding (A), satellite imagery of the area (B, C), the shoal detection product (D), and the FAB SDB product (E). No soundings are charted in or near Levasseur Inlet; a single line of soundings are charted for Admiralty Inlet (west of the area shown in Fig. 5). A shoal dominating the entrance to Levasseur Inlet is clearly visible in the satellite imagery (C), and is correctly detected by the shoal product, though with central parts of the shoal missing (not indicated as shoal). FAB SDM estimates a minimum depth of 0.3 m for the part of the shoal where the grounding occurred. The draught of the *Hanse Explorer* is 4.3 m.

3.1.4 Martin Bergmann grounding

On 03 September 2014, the *Martin Bergmann* ran aground in largely uncharted waters near Gjoa Haven, eastern Queen Maud Gulf, Nunavut, while searching for Sir John Franklin's lost ships, *HMS Erebus* and *HMS Terror*. Weather conditions during the grounding were not reported. Fig. 6 shows that the chart contains two soundings just west of the shoal that caused the grounding, but very sparse bathymetric data are charted in the area near the grounding, which contains many shoals. The shoal that caused the grounding is clearly visible in the satellite image, correctly detected in the shoal product, and the FAB SDB indicates its minimum depth as 0.3 m. With a draught of 3.43 m (Arctic Focus, 2025), knowledge of this shoal and its minimum depth would have had obvious implications for navigation of the *Martin Bergmann*.

https://doi.org/10.58440/ihr-31-2-a13

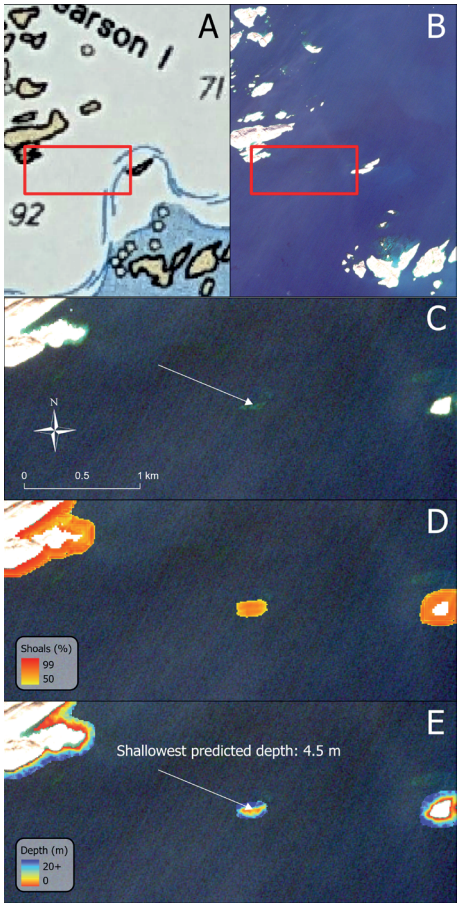


Fig. 4 Comparison of a subset of CHS chart 7502 from 1998, current at the time of grounding (A), a Sentinel-2 satellite image covering the same area (B), a section of the satellite image showing the shoal on which the grounding happened in greater detail (C), the same satellite image with the shoal detection product overlaid (D), and the same satellite image with the FAB SDB product overlaid (E). The extent of the areas shown in (C-E) is indicated by the red rectangles in (A) and (B).

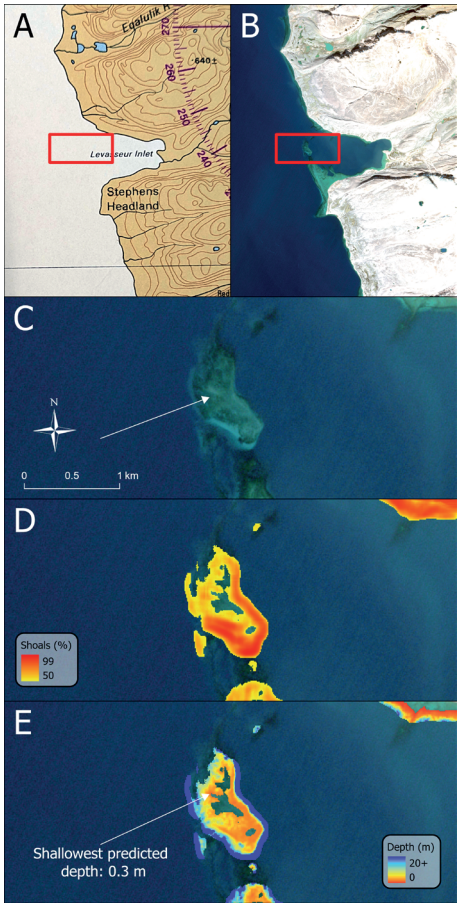


Fig. 5 Comparison of a subset of CHS chart 7568 from 1985, current at the time of grounding (A), a Sentinel-2 satellite image covering the same area (B), a section of the satellite image showing the shoal on which the grounding happened in greater detail (C), the same satellite image with the shoal detection product overlaid (D), and the same satellite image with the FAB SDB product overlaid (E). The extent of the areas shown in (C-E) is indicated by the red rectangles in (A) and (B).

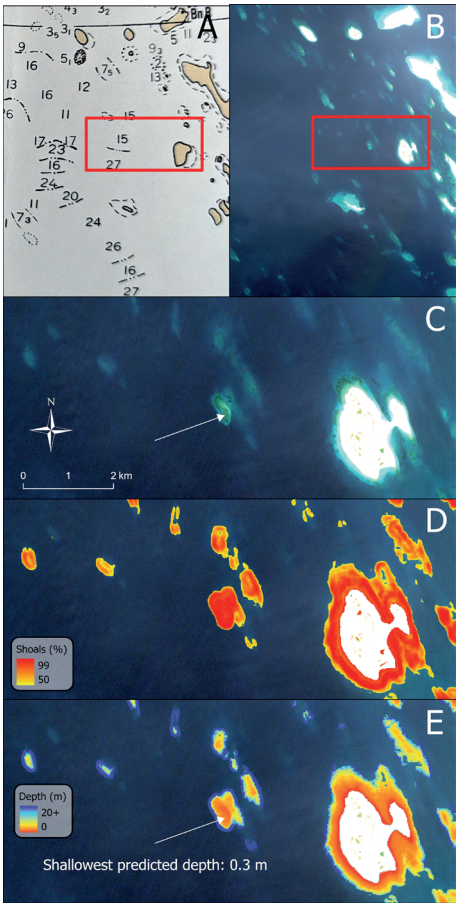


Fig. 6 Comparison of a subset of CHS chart 7083 from 1980, current at the time of grounding (A), a Sentinel-2 satellite image covering the same area (B), a section of the satellite image showing the shoal on which the grounding happened in greater detail (C), the same satellite image with the shoal detection product overlaid (D), and the same satellite image with the FAB SDB product overlaid (E). The extent of the areas shown in (C-E) is indicated by the red rectangles in (A) and (B).

3.2 SDB accuracy

Comparison between the FAB SDB estimates and survey data provided by CHS in the form of NONNA10 rasters was limited to depths up to 10 m due to the rapid degradation of SDB performance at deeper depths. This comparison, possible only for the shoals on which the *Clipper Adventurer* and *V/L Camsell* ran aground due to the limited coverage of CHS data, shows that FAB SDB performs similarly to what is reported for SDB products elsewhere in the Arctic (Ahola et al., 2020; Chénier et al., 2018). The comparison for the *Clipper Adventurer* (Fig. 7A; n = 380, R^2 = 0.58), shows a slight bias toward depth overestimation, with depths overestimated by an average of 0.71 m, and a mean absolute difference between SDB and survey data of 1.04 m. The comparison for *V/L Camsell* (Fig. 7B; n = 78, R^2 = 0.45) instead shows a slight bias toward depth underestimation, with depths underestimated by an average of 0.89 m, and a mean absolute difference between SDB and survey data of 1.35 m. Given these error statistics, the FAB SDB product would not meet International Hydrographic Organization (IHO) Order 2 specifications for vertical accuracy and would be categorized as CATZOC D data. In consequence, and as has been the practice at CHS, the FAB SDB product should not be directly used for charting. However, it is important to note that especially the comparison of FAB SDB to the CATZOC B and C survey data available for the *V/L Camsell* grounding site, and the resulting error statistics, should be interpreted considering the quality of the CHS data available for that comparison. It is possible that the relatively lower R^2 and larger MAD of the FAB SDB product at the *V/L Camsell* grounding site is due to the lower quality of the data used for comparison at this site.

4 Discussion

This study presented a review of seven groundings that occurred on shoals in the Canadian Arctic. All these shoals are clearly visible and easily detectable in satellite imagery but were not indicated on the CHS charts current at the time of each grounding. SDB applied to the satellite imagery suggests that the shallowest depths of these shoals ranged from 0.3 m to 5.1 m. In comparison, the draughts of the four vessels whose groundings were described above range

https://doi.org/10.58440/ihr-31-2-a13

between 3.43 m (*Martin Bergmann*) and 5.9 m (*Akademik Ioffe*). The first three of the groundings listed in Table 1, reported in Appendix B, occurred in 1980, 1984, and 1990, before the near-global coverage of free and publicly available satellite imagery that exists today. As a result, at the time of these groundings no satellite imagery of the shoals was publicly available. However, the shoals responsible for the remaining four groundings are clearly visible in both Landsat imagery, which has been available at 30-m spatial resolution for many areas since 1984 and has been free and publicly available since 2008 (Wulder et al., 2012), as well as in the Sentinel-2 imagery used in this study, which has been free and publicly available since 2015. It is therefore reasonable to suggest that at least the four groundings that took place since 2010 could have been avoided if the information contained in free and publicly available satellite imagery had been used to better inform mariners of the existence of these shoals. It is notable that following several of the reviewed groundings, CHS conducted detailed multi-beam surveys of the shoals and nearby areas. Although such post-incident surveys are undoubtedly beneficial for refining the relevant charts, this reactive approach misses the critical opportunity to avoid incidents entirely through proactive identification of hazards.

It is important to note that providing image-derived information to mariners does not necessarily require sophisticated image processing methods to be applied to the imagery. It should be clear to anyone looking at Figs. 3–6, as well as the figures in Appendix B, that satellite imagery inherently contains valuable information on water depth because variations in color and texture provide direct visual cues indicating the locations of shoals. Most simply, supplying mariners with satellite imagery in a format that allows it to be accessed and visualized, including while on the water, would in many cases be sufficient for route planning and hazard avoidance. Additional products, such as the ones shown in this study, should ideally accompany the imagery. In addition to the shoal detection product used in this study, examples of similar products include EOMAP's shoals database (EOMAP, 2023) and the StayAway product (ChartWorld, 2025). Several SDB products are also available, including Liquid Geomatics's FAB SDB used here, and similar products provided either commercially or by hydrographic offices. It is clear that products derived from satellite imagery cannot and should not replace the charts and other documents that are legally required for vessels operating in Canadian waters (DFO, 2020) or elsewhere; rather, satellite imagery and products derived from it can provide additional information on hazards that are not shown on those charts.

The continued occurrence of groundings in uncharted or poorly surveyed waters underscores the need to make better use of satellite-derived information in some form. The question is how best to make use of the information contained in the imagery. In

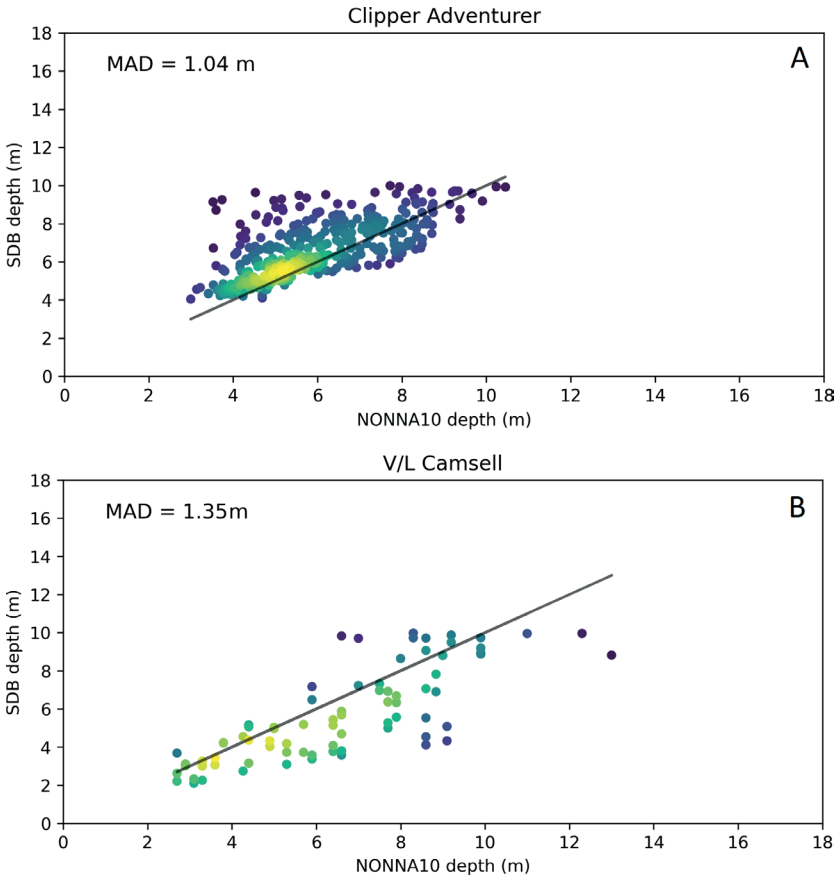


Fig. 7 Scatter plots comparing bathymetry estimates from FAB SDB (y-axes) to NONNA10 bathymetry data from CHS (x-axes) for the two groundings sites for which data were available: the site of the *Clipper Adventurer* (A) and *V/L Camsell* (B).

2021 IHO established an SDB project team that has produced a guidance document (IHO, 2024) providing "technical best practices and guidelines" for SDB. This may help guide the use of satellite imagery for SDB and facilitate international discussions of its appropriate use. SDB is gradually finding its way onto charts, including in France, the United Kingdom, the United States, and Canada (Chénier et al., 2018), where the CHS has established a Remote Sensing Centre of Excellence (RSCoE) to accelerate the use satellite imagery in hydrography, including for SDB purposes (Chénier et al., 2020). Where SDB products are of sufficient quality integration on charts is often the best solution, but SDB products are limited in coverage to relatively shallow depths, and their errors increase with the depth of water (Duan et al., 2022; Knudby & Richardson, 2023) until the seafloor becomes undetectable, at which point SDB estimates are no longer meaningful. SDB products should thus not blindly be included on charts; indeed, the SDB errors reported here for the two shoals for which reference data were available for comparison may be deemed unacceptable for inclusion on charts.

Yet there is no doubt that the imagery contains real and valuable information on the location of shoals. As of April 2025, CHS is exploring the use of automated shoal detection with an approach similar to the one used in this study, testing its ability to

https://doi.org/10.58440/ihr-31-2-a13

both validate SDB results and delineate hazards to navigation for production of navigational warnings (NAVWARNs) and notices to mariners (NOTMARs). Where the quality of SDB products is deemed insufficient for direct inclusion on charts, the IHO's S-100 universal hydrographic data model may also provide other avenues for inclusion of information derived from satellite imagery. SDB data products could be included under S-102 (Bathymetric Surface), a raster product designed to represent bathymetric depths, and identified shoals could be included under S-124 (Navigational Warnings), a vector product intended to provide information on the nature and extent of navigational warnings. No S-100 data product seems suitable to hold the imagery itself; development of such a product could be beneficial and should be considered. In summary, despite useful satellite imagery having been freely available since 2008, many nautical charts continue to contain nothing but white space in areas where shoals are clearly visible in the imagery. This results in needless groundings, including the four reviewed in this study that occurred since 2010. This situation highlights the need for a paradigm shift in the utilization of satellite imagery within the hydrographic community. Such a shift is already under way, but with a rapidly warming Arctic and its associated increase in vessel traffic, it is imperative to further accelerate the use of satellite imagery to extract information on the location of shoals and, where possible, their approximate depth, and to provide such information to mariners in the form that is most useful to them.

5 Conclusion

This study has demonstrated that several recent vessel groundings in the Canadian Arctic might have been prevented if mariners had been provided with satellite-derived information on the locations of shoals that were not indicated on the official charts at the time. It is the responsibility of the hydrographic community to produce data products that improve the safety of navigation for mariners. Satellite imagery contains valuable information that can be used for this purpose; specifically, it contains clear visual cues that enable identification of shoal locations and estimation of water depth. In unsurveyed or poorly surveyed regions of the world, such information may be the best that is available. Given the rapidly warming Arctic Ocean and the corresponding increase in vessel traffic, proactive use of satellite imagery in this inadequately surveyed region, rather than reactive multi-beam surveys conducted after groundings have already occurred, would significantly improve the safety of navigation. Vessel groundings have serious financial, environmental, and safety consequences, including potential loss of life. It is imperative for the hydrographic community to incorporate satellite imagery proactively to improve navigational safety in poorly surveyed waters.

Acknowledgements

Development of the FAB SDB workflow began in 2018 after discussions with Dr. John Hedley about the possibility of fully automating physics-based SDB. Since then, it has been continuously refined with input and inspiration from numerous people. Funding for its development has been provided by the Canadian Space Agency (22AO2-LIQU). The model that differentiates optically shallow and optically deep water, which is the basis for the shoal detection product, was developed mostly by a group of students at the University of Ottawa: Galen Richardson, Neve Foreman, Yulun Wu, and Yiwen Lin. The idea for the present paper was inspired by discussion with several other colleagues who prefer to remain anonymous. The initial manuscript was improved on the basis of very constructive comments from three anonymous reviewers

References

Ahola, R., Chénier, R., Sagram, M. and Horner, B. (2020). The impact of sensors for satellite derived bathymetry within the Canadian Arctic. *Geomatica, 74*, pp. 46–64.

Arctic Focus (2025). *R/V Martin Bergmann*. Arctic Focus. https://www.arcticfocus.org/about/vessels-and-labs/rv-martin-bergmann/ (last accessed 27 July 2025).

Caballero, I. and Stumpf, R. P. (2023). Confronting turbidity, the major challenge for satellite-derived coastal bathymetry. *Science of the Total Environment, 870*, 161898.

Carrere, L., Lyard, F., Cancet, M. and Guillot, A. (2015). FES 2014, a new tidal model on the global ocean with enhanced accuracy in shallow seas and in the Arctic region. *Geophysical Research Abstracts, 17*, 5481.

Casal, G., Hedley, J. D., Monteys, X., Harris, P., Cahalane, C. and McCarthy, T. (2020). Satellite-derived bathymetry in optically complex waters using a model inversion approach and Sentinel-2 data. *Estuarine and Coastal Shelf Science, 241*, 106814.

ChartWorld (2025). *StayAway service complements ENC Depth Information*. ChartWorld. https://www.chartworld.com/web/news/stayaway-service-complements-enc-depth-information/ (last accessed 19 March 2025).

Chénier, R., Faucher, M.-A. and Ahola, R. (2018). Satellite-Derived Bathymetry for Improving Canadian Hydrographic Service Charts. *ISPRS International Journal of Geo-Information, 7*, 306.

Chénier, R., Omari, K., Blondel, E., Sagram, M. and Jirovec, A. (2020). Accelerating the usage of earth and oceans observation data in hydrographic applications. *The International Hydrographic Review, 30*, pp. 103–127. CHS (2024). *Canadian Hydrographic Service Non-Navigational (NONNA) Bathymetric Data*. Open Government Portal. https://open.canada.ca/data/en/dataset/d3881c4c-650d-4070-bf9b-1e00aabf0a1d (last accessed 6 March 2025).

CHS (2023). *Arctic charting*. Canadian Hydrographic Service. https://www.charts.gc.ca/arctic-arctique/index-eng.html (last accessed 25 February 2025).

https://doi.org/10.58440/ihr-31-2-a13

Council of Canadian Academies (2016). *Commercial Marine Shipping Accidents: Understanding the Risks in Canada*. Council of Canadian Academies. Ottawa, Canada.

Dalton, A. (2023). *Identifying Iceberg Production Processes, Drift Patterns and Coexistence with Ships in the Eastern Canadian Arctic* [PhD thesis, Université d'Ottawa / University of Ottawa].

Daly, C., Baba, W., Bergsma, E., Thoumyre, G., Almar, R. and Garlan, T. (2022). The new era of regional coastal bathymetry from space: A showcase for West Africa using optical Sentinel-2 imagery. *Remote Sensing of Environment, 278*, 113084.

Dawson, J., Pizzolato, L., Howell, S. E. L., Copland, L. and Johnston, M. E. (2018). Temporal and Spatial Patterns of Ship Traffic in the Canadian Arctic from 1990 to 2015. *ARCTIC, 71*, pp. 15–26.

Dekker, A. G., Phinn, S. R., Anstee, J., Bissett, P., Brando, V. E., Casey, B., Fearns, P., Hedley, J., Klonowski, W., Lee, Z. P., Lynch, M., Lyons, M., Mobley, C. and Roelfsema, C. (2011). Intercomparison of shallow water bathymetry, hydro-optics and benthos mapping techniques in Australian and Caribbean coastal environments. *Limnology & Oceanography Methods, 9*, pp. 396–425.

DFO (2020). *Navigation Safety Regulations. Government of Canada*. https://lois.justice.gc.ca/eng/regulations/SOR-2020-216/index.html (last accessed 19 March 2025).

Duan, Z., Chu, S., Cheng, L., Ji, C., Li, M. and Shen, W. (2022). Satellite-derived bathymetry using Landsat-8 and Sentinel-2A images: assessment of atmospheric correction algorithms and depth derivation models in shallow waters. *Optics Express, 30*, pp. 3238–3261.

Emde, C., Buras-Schnell, R., Kylling, A., Mayer, B., Gasteiger, J., Hamann, U., Kylling, J., Richter, B., Pause, C., Dowling, T. and Bugliaro, L. (2016). The libRadtran software package for radiative transfer calculations (version 2.0.1). *Geoscientific Model Development, 9*, pp. pp. 1647–1672.

EOMAP (2023). Shoals Database. EOMAP. https://www.eomap.com/*shoals-database/* (last accessed 19 March 2025).

Government of Canada (2014). *Fall Report of the Commissioner of the Environment and Sustainable Development*. Office of the Auditor General of Canada. Ottawa, Canada.

Hedley, J., Roelfsema, C., Koetz, B. and Phinn, S. (2012). Capability of the Sentinel 2 mission for tropical coral reef mapping and coral bleaching detection. *Remote Sensing of Environment, 120*, pp. 145–155.

Hedley, J., Roelfsema, C. and Phinn, S. R. (2009). Efficient radiative transfer model inversion for remote sensing applications. *Remote Sensing of Environment, 113,* pp. 2527–2532.

Hedley, J. D. (2019). *Image Data Analysis (IDA) software*. Numerical Optics, Tiverton, UK.

Hedley, J. D. (2018). Atmospheric correction of Sentinel-2 and Landsat 8 for satellite derived bathymetry. *Ocean Optics XXIV, Dubrovnik, Croatia.*

Hedley, J. D., Roelfsema, C. and Phinn, S.R. (2010). Propagating uncertainty through a shallow water mapping algorithm based on radiative transfer model inversion. *Ocean Optics XX, Anchorage, USA.*

Hodúl, M., Bird, S., Knudby, A. and Chénier, R. (2018). Satellite derived photogrammetric bathymetry. *ISPRS Journal of Photogrammetry and Remote Sensing, 142*, pp. 268–277.

Hodúl, M., Chénier, R., Faucher, M.-A., Ahola, R., Knudby, A. and Bird, S. (2020). Photogrammetric Bathymetry for the Canadian Arctic. *Marine Geodesy, 43*, pp. 23–43.

Howell, S. E. L., Babb, D. G., Landy, J. C., Glissenaar, I. A., McNeil, K., Montpetit, B. and Brady, M. (2024). Sea ice transport and replenishment across and within the Canadian Arctic Archipelago, 2016–2022. *The Cryosphere, 18,* pp. 2321–2333.

IHO (2024). *B-13 Satellite-Derived Bathymetry Best Practice Guide*. International Hydrographic Organization (IHO), Monaco.

Ilori, C. O. and Knudby, A. (2020). An Approach to Minimize Atmospheric Correction Error and Improve Physics-Based Satellite-Derived Bathymetry in a Coastal Environment. *Remote Sensing, 12*, 2752.

Ilori, C. O., Pahlevan, N. and Knudby, A. (2019). Analyzing Performances of Different Atmospheric Correction Techniques for Landsat 8: Application for Coastal Remote Sensing. *Remote Sensing, 11*, 469.

Kim, Y.-H., Min, S.-K., Gillett, N. P., Notz, D. and Malinina, E. (2023). Observationally-constrained projections of an ice-free Arctic even under a low emission scenario. *Nature Communications, 14*, 3139.

Knudby, A., Ahmad, S. K. and Ilori, C. (2016). The potential for Landsat-based bathymetry in Canada. *Canadian Journal of Remote Sensing, 42*, pp. 367–378.

Knudby, A. and Richardson, G. (2023). Incorporation of neighborhood information improves performance of SDB models. *Remote Sensing Applications: Society and Environment, 32*, 101033.

Lasserre, F. and Baudu, H. (2024). *Navigation in the Arctic in 2024, The Arctic Review.* Observatoire de la politique et la sécurité de l'arctique (OPSA), Québec, Canada.

Lee, Z., Carder, K. L., Mobley, C. D., Steward, R. G. and Patch, J. S. (1999). Hyperspectral remote sensing for shallow waters: 2. Deriving bottom depths and water properties by optimization. *Applied Optics, 38*, pp. 3831–3843.

Lee, Z., Carder, K. L., Mobley, C. D., Steward, R. G., Patch, J. S., 1998. Hyperspectral remote sensing for shallow waters. I. A semianalytical model. *Applied Optics, 37*, pp. 6329–6338.

Liu, Y., Luo, H., Min, C., Chen, Q. and Yang, Q., (2024). Changes in the Arctic Traffic Occupancy and Their Connection to Sea Ice Conditions from 2015 to 2020. *Remote Sensing, 16*, 1157.

Lyard, F. H., Allain, D.J., Cancet, M., Carrère, L. and Picot, N. (2021). FES2014 global ocean tide atlas: design and performance. *Ocean Science, 17*, pp. 615–649.

Lyzenga, D. R. (1985). Shallow-water bathymetry using combined lidar and passive multispectral scanner data. *International Journal of Remote Sensing, 6*, pp. 115–125.

Lyzenga, D. R. (1978). Passive remote sensing techniques for mapping water depth and bottom features. *Applied Optics, 17*, pp. 379–383.

Mavraeidopoulos, A., Pallikaris, A. and Oikonomou, E. (2017). Satellite Derived Bathymetry (SDB) and safety of navigation. *The International Hydrographic Review, 17*.

Nicoll, A., Dawson, J., Marty, J., Copland, L. and Sawada, M. (2024). Analysis of shipping accident patterns among commercial and non-commercial vessels operating in ice-infested waters in Arctic Canada from 1990 to 2022. *Journal of Transportation Geography, 121*, 104046.

NOAA, NASA and USAF (1976). *U.S. Standard Atmosphere, 1976*. National Oceanic and Atmospheric Administration, National Aeronautics and Space Administration, United States Air Force, Washington, USA.

Richardson, G., Foreman, N., Knudby, A., Wu, Y. and Lin, Y. (2024). Global deep learning model for delineation of optically shallow and optically deep water in Sentinel-2 imagery. *Remote Sensing of Environment, 311*, 114302.

Robin, C., Nudds, S., MacAulay, P., Godin, A., De Lange Boom, B. and Bartlett, J. (2016). Hydrographic Vertical Separation Surfaces (HyVSEPs) for the Tidal Waters of Canada. *Marine Geodesy, 39*, pp. 195–222.

Stumpf, R. P., Holderied, K. and Sinclair, M. (2003). Determination of water depth with high-resolution satellite imagery over variable bottom types. *Limnology and Oceanography, 48*, pp. 547–556.

Trémas, T. L., Déchoz, C., Lacherade, S., Nosavan, J. and Petrucci, B. (2015). Sentinel-2: presentation of the CAL/VAL commissioning phase. Proceedings of the Image and Signal *Processing for Remote Sensing XXI conference, SPIE*, pp. 94–106.

TSB (2010). *Marine Investigation Report M10H0006*. Transportation Safety Board of Canada, Ottawa, Canada.

TSB (2021). *Marine transportation safety investigation report M18C0225*. Transportation Safety Board of Canada, Ottawa, Canada.

TSB (2025). *Data and statistics on marine transportation occurrences*. Transportation Safety Board of Canada. https://www.tsb.gc.ca/eng/stats/marine/index.html (last accessed 25 February 2025).

Wulder, M. A., Masek, J. G., Cohen, W. B., Loveland, T. R. and Woodcock, C. E. (2012). Opening the archive: How free data has enabled the science and monitoring promise of Landsat. *Remote Sensing of Environment, 122*, pp. 2–10.

Yadav, J., Kumar, A. and Mohan, R. (2020). Dramatic decline of Arctic Sea ice linked to global warming. *Natural Hazards, 103*, pp. 2617–2621.

Zhu, Z., Wang, S. and Woodcock, C. E. (2015). Improvement and expansion of the Fmask algorithm: cloud, cloud shadow and snow detection for Landsats 4–7, 8 and Sentinel 2 images. *Remote Sensing of Environment, 159*, pp. 269–277.

Appendix A: Additional details on the FAB SDB workflow

A.1 Masking

After downloading all Sentinel-2 images, all pixels with top-of-atmosphere (TOA) reflectance >1.5 % in the shortwave infrared (SWIR; band 12) are masked out; this threshold has been determined from testing on >100 images globally. Initially the internal cloud flags for each sensor were tested for this purpose, as was the Fmask algorithm (Zhu et al., 2015), but both produced generally poor results over coastal areas. In addition to masking out clouds, a simple SWIR-based threshold also serves to mask out land, sea ice, vessels, white caps and pixels with excessive sunglint, all of which are undesirable for SDB and detectable by increased SWIR reflectance. In addition to these masks developed for each image, a land mask is created by masking out all pixels with less than three unmasked observations across all images for the area. This is done to ensure that pixels that were masked out in most images, but remained unmasked once or twice, were excluded from further processing (Fig. 8).

A.2 Deep-water detection and atmospheric correction

Atmospheric correction in FAB is based on deep-water reference polygons, 24 of which are identified for each tile. To do so, all available images are combined to calculate the per-pixel median unmasked TOA reflectance in the 490-nm band. A 1000 m × 1000 m mean filter is applied

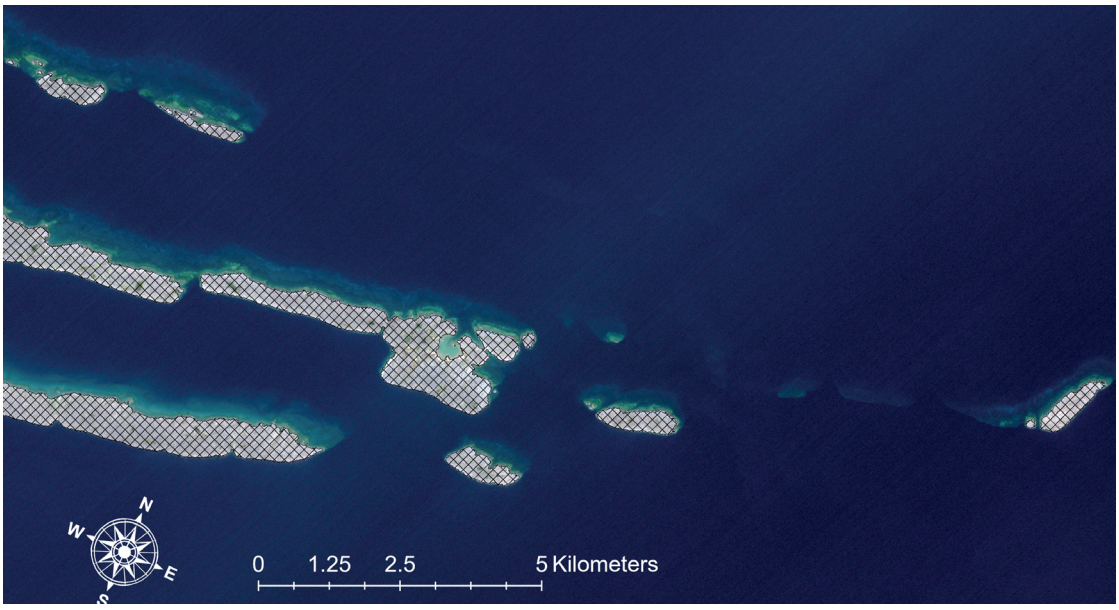


Fig. 8 An example of the land mask applied to satellite imagery covering the area surrounding the 2010 grounding of the Clipper Adventurer. Masked-out pixels are shown with cross-hatching.

https://doi.org/10.58440/ihr-31-2-a13

to the result to reduce noise; this also serves to make pixels close to land less likely to be identified as deep water. Pixels that are unmasked in less than three images, or located within 500 m of the tile edge, as well as pixels that do not connect through other valid pixels to the tile edge (i.e. lakes) are then removed. The resulting data layer is divided into four quadrats, and within each quadrat six random pixels, selected among those with values less than or equal to 1.5 times the darkest unmasked pixel, are randomly selected as the centers of 1000 m × 1000 m deep-water areas.

Atmospheric correction is then performed with the deep-water calibration (DWC) method implemented in the IDA software (Casal et al., 2020; Hedley, 2019, 2018). The DWC method is based on look-up tables of atmospheric reflectance and transmission calculated with libRadtran (Emde et al., 2016) using the US standard atmosphere model (NOAA et al., 1976) and a maritime 99 % relative humidity aerosol model (MAR99) parameterized with scene-averaged sun and view angles. The atmospheric correction requires specifying aerosol optical thickness at 550 nm (τ550), and wind speed (u10). The wind speed term is effectively a proxy for the spatially averaged residual sun glint, dependent on the solar-view geometry. While the values of these two parameters can be estimated with auxiliary data, the DWC method instead utilizes the deep-water areas identified above, in combination with the bathymetry model described below, to estimate the values of τ550 and u10 that will lead to water depth estimates of at least 15 m for the deep-water areas. In consequence, the estimated τ550 and u10 values may not be correct for each image, but they ensure that deep water will be correctly identified as deep in the bathymetry estimation.

A.3 Bathymetry estimation

Per-pixel water depth is estimated for all atmospherically corrected images using the RTM inversion implemented in IDA. This approach is based on least-squares matching between the above-water remote sensing reflectance (R_{rs}) observed in each pixel and a look-up table containing R_{rs} values forward-modeled for a range of water depth, water quality and seafloor reflectance parameters. This forward modeling is based on the semi-analytical model developed by Lee et al. (1999, 1998), which takes the general form:

$$R_{rs}(\lambda) = f(P, G, X, H, e, \Theta_s, \Theta_v, \lambda) \quad (1)$$

In Eq. 1, *P*, *G*, and *X* are proxies for the amount of phytoplankton (mg m^{-3}), absorption at 440 nm due to coloured dissolved organic matter (CDOM; m^{-1}), and backscattering at 440 nm due to suspended sediment (m^{-1}), respectively, *H* is the water depth (m), *e* is the seafloor reflectance (unitless), Θ_s is the solar zenith angle, and Θ_v is the viewing zenith angle. λ (henceforth omitted for simplicity) is the wavelength. This forward model is specified for each image, using default value ranges for *P*, *G*, *X*, and *H* (Table 2), linear mixes of two default seafloor reflectance spectra as *e*, and image-specific values of Θs and Θv.

Table 2 Default value ranges for forward modeling of R_{rs}.

Variable	*P*	*G*	*X*	*H*
Minimum	0	0	0	0
Maximum	2	0.2	0.1	30

FAB processes an image by inverting this forward model: an Adaptive Look-Up Table (ALUT; Hedley et al., 2009) with approximately 10^6 entries is built and then searched using the Binary Space Partitioning approach (BSP; Hedley et al., 2009) to estimate H for a given R_{rs}. This ALUT search is not applied directly to the R_{rs} values; rather an uncertainty propagation is performed by inverting each R_{rs} spectrum 20 times, each time after adding a random spectrally correlated noise term derived from the covariance matrix of pixels from the deep-water areas (Hedley et al., 2010; Knudby et al., 2016). Water depth at the time of image acquisition is then estimated for each pixel as the mean water depth value from those 20 inversions.

A.4 Vertical referencing and post-processing

The estimated depths for each image are vertically referenced to mean sea level (MSL) by correcting for tidal level at the time of image acquisition using the FES2014 global tide model (Carrere et al., 2015; Lyard et al., 2021) and then referenced to chart datum using a vertical separation model provided by CHS (Robin et al., 2016). CHS uses Lower Low Water, Large Tide (LLWLT), as the vertical datum for most of its coastal charts. An ensemble bathymetry estimate is produced by calculating the median unmasked per-pixel water depth from all images (Ilori & Knudby, 2020) and applying a 3 × 3 mean filter to the result. Finally deep water is masked out from this bathymetry estimate by applying the FAB SDB estimates only to pixels deemed optically shallow (see Section 2.3).

Appendix B: Additional groundings

This appendix contains the case studies for the groundings that occurred prior to 2010, before the availability of Sentinel-2 satellite imagery, and before the availability of free and publicly available Landsat imagery. A review of the Landsat image archives did not yield any satellite imagery in which these shoals were visible prior to the time of each grounding.

B.1 TSB Occurrence ID 4287

In the morning of 31 August 1980, a vessel (name unknown) ran aground under power and sustained damage near Gunnar's Island in Baumann Fiord, Nunavut, during clear weather, low wind and smooth sea state. Fig. 9 shows that the chart indicated a sounding of 24 m depth nearby, but did not indicate the presence of the shoal that caused the grounding. The shoal is clearly visible in the satellite image, correctly detected by the shoal product, and FAB SDB indicated its minimum depth as 5.1 m.

B.2 TSB Occurrence ID 9351

On 25 August 1984, *V/L Camsell* ran aground under power and sustained damage near Wiik Island in Storis Passage, eastern Queen Maud Gulf, Nunavut, during clear weather, low wind and smooth sea state. The TSB report indicates that the vessel "proceeded slowly in area of incomplete soundings". Fig. 10 shows that the chart contains several soundings near the shoal that caused the grounding, the nearest of which indicates a depth of 5.2 m. The shoal is clearly visible in the satellite image, correctly detected by the shoal product, and FAB SDB indicated its minimum depth as 1.9 m.

B.3 TSB Occurrence ID 18332

On 24 August 1990, a vessel (name unknown) reported bottom contact while on a Search and Rescue (SAR) in largely uncharted waters near O'Reilly Island south of Storis Passage, eastern Queen Maud Gulf, Nunavut, during clear weather and with light ice cover. Fig. 11 shows that the chart contains a line of soundings just west of the shoal that caused the grounding, but very sparse bathymetric data are charted in the general area of the grounding, which contains many shoals. The shoal that caused the grounding is clearly visible in the satellite image, correctly detected by the shoal product, and FAB SDB indicated its minimum depth as 1.3 m. Note that the TSB reports the grounding location in between several shoals visible in the satellite imagery (Fig. 11); the 1.3 m depth estimated by FAB SDB refers to the shoal located northwest of the reported grounding location.

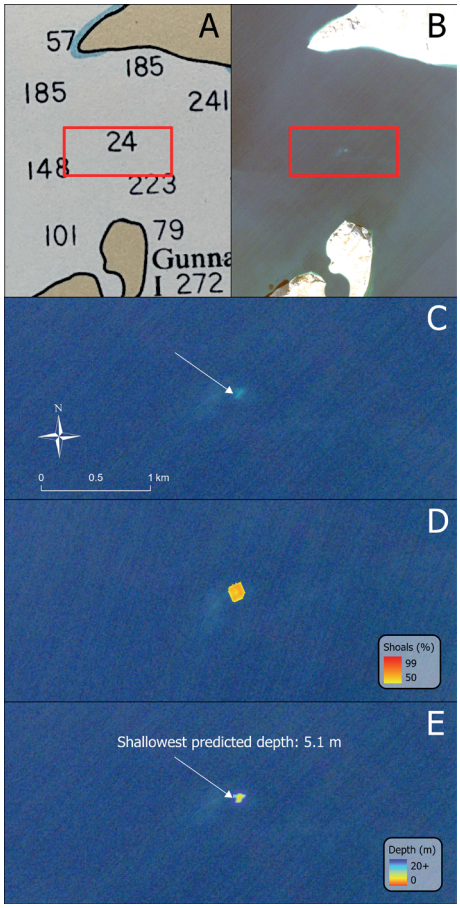


Fig. 9 Comparison of a subset of CHS chart 7590 from 1974, current at the time of grounding (A), a Sentinel-2 satellite image covering the same area (B), a section of the satellite image showing the shoal on which the grounding happened in greater detail (C), the same satellite image with the shoal detection product overlaid (D), and the same satellite image with the FAB SDB product overlaid (E). The extent of the areas shown in (C-E) is indicated by the red rectangles in (A) and (B).

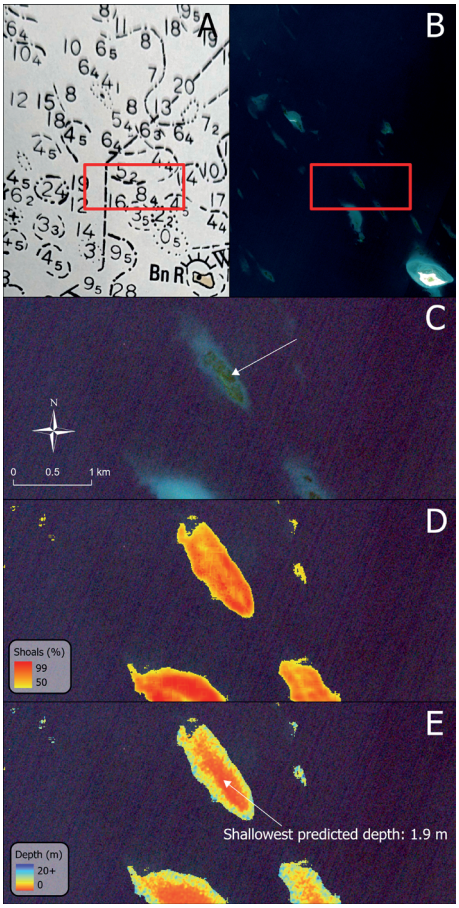


Fig. 10 Comparison of a subset of CHS chart 7083 from 1980, current at the time of grounding (A), a Sentinel-2 satellite image covering the same area (B), a section of the satellite image showing the shoal on which the grounding happened in greater detail (C), the same satellite image with the shoal detection product overlaid (D), and the same satellite image with the FAB SDB product overlaid (E). The extent of the areas shown in (C-E) is indicated by the red rectangles in (A) and (B).

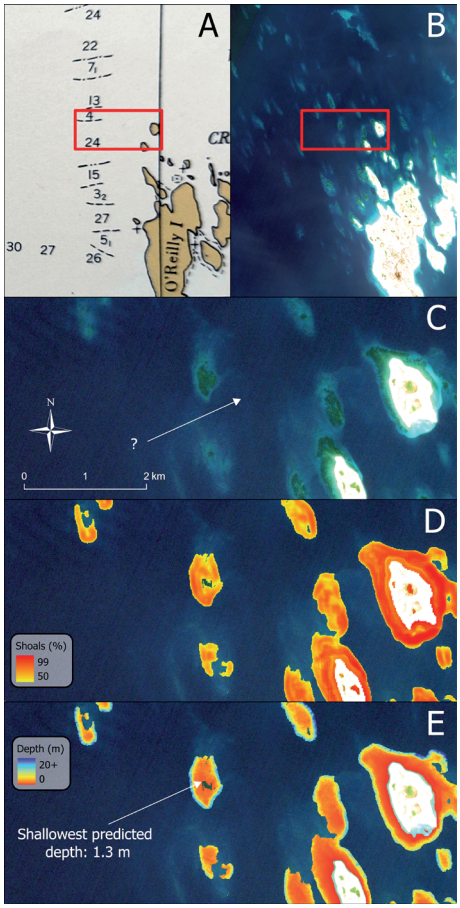


Fig. 11 Comparison of a subset of CHS chart 7083 from 1980, current at the time of grounding (A), a Sentinel-2 satellite image covering the same area (B), a section of the satellite image showing the shoal on which the grounding happened in greater detail (C), the same satellite image with the shoal detection product overlaid (D), and the same satellite image with the FAB SDB product overlaid (E). The extent of the areas shown in (C-E) is indicated by the red rectangles in (A) and (B).

https://doi.org/10.58440/ihr-31-2-a13

Author's biography

Dr. Anders Knudby is a Professor at the University of Ottawa, where he directs the Shallow-Water Earth Observation Laboratory (https://www.shallowwaterlab.com/). He is also the Principal Scientist at Liquid Geomatics Ltd. (https://www.liquidgeomatics.ca/). Having worked with satellite remote sensing for over 25 years, he has broad experience with optical satellite image processing and applied earth observation, and has specific expertise in aquatic remote sensing. He has worked with satellite-derived bathymetry for over a decade. Dr. Knudby is the University of Ottawa's representative with the Canada Ocean Mapping Research and Education Network (COMREN; https://oceanmapping.ca/), and on the steering committee of NetCOLOR, the network of Canadian experts and end-users in the field of aquatic color remote sensing (https://www.netcolor.ca/).



Anders Knudby

https://doi.org/10.58440/ihr-31-2-a13